Acta Crystallographica Section C
Crystal Structure Communications
ISSN 0108-2701

Copper(II) bromide and copper(II) acetate complexes of 4,4′-(*p*-phenylene)bipyridazine

Anna S. Degtyarenko,[a] Pavlo V. Solntsev,[a] Eduard B. Rusanov,[b] Alexander N. Chernega[b] and Konstantin V. Domasevitch[a]*

[a]Inorganic Chemistry Department, Kiev University, Volodimirska Street 64, Kiev 01033, Ukraine, and [b]Institute of Organic Chemistry, Murmanskaya Street 5, Kiev 02094, Ukraine
Correspondence e-mail: dk@univ.kiev.ua

Received 2 June 2008
Accepted 11 June 2008
Online 21 June 2008

4,4′-(*p*-Phenylene)bipyridazine, $C_{14}H_{10}N_4$, (I), and the coordination compounds *catena*-poly[[dibromidocopper(II)]-μ-4,4′-(*p*-phenylene)bipyridazine-κ^2N^2:$N^{2'}$], $[CuBr_2(C_{14}H_{10}N_4)]_n$, (II), and *catena*-poly[[[tetrakis(μ-acetato-κ^2O:O')dicopper(II)]-μ-4,4′-(*p*-phenylene)bipyridazine-κ^2N^1:$N^{1'}$] chloroform disolvate], $\{[Cu_2(C_2H_3O_2)_4(C_{14}H_{10}N_4)]\cdot 2CHCl_3\}_n$, (III), contain a new extended bitopic ligand. The combination of the *p*-phenylene spacer and the electron-deficient pyridazine rings precludes C—H$\cdots\pi$ interactions between the lengthy aromatic molecules, which could be suited for the synthesis of open-framework coordination polymers. In (I), the molecules are situated across a center of inversion and display a set of very weak intermolecular C—H$\cdots$N hydrogen bonds [3.399 (3) and 3.608 (2) Å]. In (II) and (III), the ligand molecules are situated across a center of inversion and act as N^2,$N^{2'}$-bidentate [in (II)] and N^1,$N^{1'}$-bidentate [in (III)] long-distance bridges between the metal ions, leading to the formation of coordination chains [Cu—N = 2.005 (3) Å in (II) and 2.199 (2) Å in (III)]. In (II), the copper ion lies on a center of inversion and adopts CuN_2Br_4 (4+2)-coordination involving two long axial Cu—Br bonds [3.2421 (4) Å]. In (III), the copper ion has a tetragonal pyramidal CuO_4N environment. The uncoordinated pyridazine N atom and two acetate O atoms provide a multiple acceptor site for accommodation of a chloroform solvent molecule by trifurcated hydrogen bonding [C—H$\cdots$O(N) = 3.298 (5)–3.541 (4) Å].

Comment

In coordination compounds, N^1,N^2-bidentate pyridazine typically sustains short-distance bridges between metal ions and supports the generation of complicated polynuclear and polymeric metal–organic motifs (Otieno *et al.*, 1995). Such arrays are interesting in view of strong magnetic coupling between the paramagnetic centers through pyridazine bridges (Carlucci *et al.*, 1994) and also as coordination subtopologies for metal–organic frameworks (Domasevitch, Solntsev *et al.*, 2007). In this way, multifunctional pyridazine N-atom donors offer a new potential for the design of solid-state coordination architecture, as was revealed by examination of the simpler bitopic ligand 4,4′-bipyridazine (Domasevitch, Gural'skiy *et al.*, 2007). The latter combines inherent abilities for coordination of closely situated metal ions (3.2 Å) and long-distance bridging at *ca* 11 Å. Extension of the effective length of the ligand is relevant for the connection of even more distant metal ions and it is an essential prerequisite for the preparation of open metal–organic frameworks. These possibilities may be anticipated for a series of new extended ligands, which unite two pyridazine functions separated by a rigid covalent spacer, *i.e.* *p*-phenylene. Such species are readily accessible *via* the inverse electron demand Diels–Alder cycloaddition of 1,2,4,5-tetrazine (Sauer *et al.*, 1998), and they may be viewed as new attractive 'building blocks' for crystal design. We report here the structure of the hitherto unknown ligand 4,4′-(*p*-phenylene)bipyridazine, (I), and two new copper(II) complexes, (II) and (III), which feature two different bidentate coordination modes.

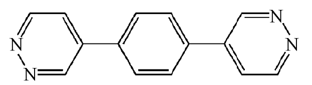
(I)

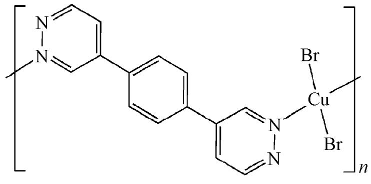
(II)

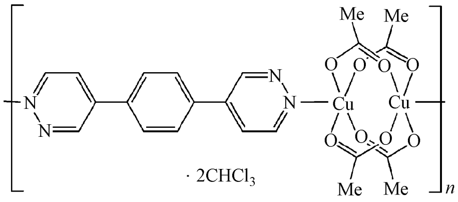
(III)

The asymmetric unit of (I) comprises a half-molecule of 4,4′-(*p*-phenylene)bipyridazine lying across a center of inversion (Fig. 1). The geometry of the heteroaromatic ring is consistent with the structure of pyridazine itself (Blake & Rankin, 1991). In the molecule of (I), the two pyridazine rings are coplanar, while exhibiting a significant twist angle of 43.15 (9)° with respect to the plane of the phenylene spacer. This suggests conformational flexibility of the molecule and a lack of conjugation between the hetero- and carbocyclic fragments, as is indicated also by the standard length of the C2—C5 bond [1.482 (2) Å]. The corresponding torsion angle

doi:10.1107/S0108270108017666

[C1—C2—C5—C6 = −43.1 (3)°] appreciably exceeds the value for terphenyl (14.4°; Baudour *et al.*, 1986), but it is consistent with a molecular geometry optimization (37.6°) performed using density function theory with the 6–311(d,p) basis set and the B3LYP hybrid functional defined in *GAMESS* (Schmidt *et al.*, 1993).

In the crystal structure of (I), the molecules associate *via* a set of very weak interactions, namely C—H···N hydrogen bonding (Table 2) and π–π contacts. A pair of C4—H4···N1^{i} bonds connects the molecules into centrosymmetric dimers, similar to those observed for unsubstituted pyridazine (Blake & Rankin, 1991), and C3—H3···N2^{ii} interactions extend this motif along the *a*-axis direction with the formation of a layer parallel to the $(02\overline{1})$ plane [symmetry codes: (i) $-x+1, -y+1, -z-1$; (ii) $x+1, y, z$; Fig. 2]. Weak slipped π–π stacking occurs between a pair of antiparallel pyridazine rings related by inversion (symmetry code: $-x+1, -y+1, -z$). The parameters of this interaction [the interplanar and inter-centroid distances are 3.4683 (11) and 3.564 (2) Å, respectively, and the slippage angle is 13.31 (8)°] are characteristic of weak π–π contacts of electron-deficient heteroaromatic rings (Janiak, 2000).

In the copper(II) complexes (II) and (III), the primary connectivity exists in the form of one-dimensional coordination chains supported by bridging of the ligand between the copper ions. In both structures, the molecules of the ligand are situated across a center of inversion, and therefore they adopt symmetric *N*,*N*′-bidentate bridging modes, while each of the pyridazine rings is coordinated in a monodentate manner. This is consistent with the coordination preferences of the simpler 4,4′-bipyridazine ligand, which is an efficient tetradentate linker towards silver(I) ions (Domasevitch, Solntsev *et al.*, 2007) but is typically bidentate towards Cu^{2+} and Zn^{2+} ions (Domasevitch, Gural'skiy *et al.*, 2007). The coordination modes in (II) and (III), however, are different, namely $N^2,N^{2'}$- and linear $N^1,N^{1'}$-coordinations, respectively. This may reflect the adaptability of the ligand to the demands of the crystal packing.

In (II), the copper ion is situated on a center of inversion and displays Jahn–Teller-distorted octahedral (4+2)-coordination, with a *trans*-CuN_2Br_2 equatorial plane [Cu1—Br1 = 2.4151 (4) Å; Fig. 3]; the octahedron is completed by two very long axial contacts [Cu1···Br1^{i} = 3.2421 (4) Å; symmetry code: (i) $-x+1, -y, -z$]. These weak bonds connect linear Br—Cu—Br units into a chain of vertex-sharing Cu_2Br_2 rhombs running along the *a*-axis direction, and overall this generates coordination layers that lie parallel to the *ab* plane (Fig. 4). These features are analogous to the situation in dibromidodipyridinecopper(II) (Cu—Br = 2.451 and 3.240 Å; Morosin, 1975), while shorter chloride bridges are essential for stabilization of the bidentate coordination of pyridazine in the copper(II)–chloride complex (Fetzer *et al.*, 1990). The axial

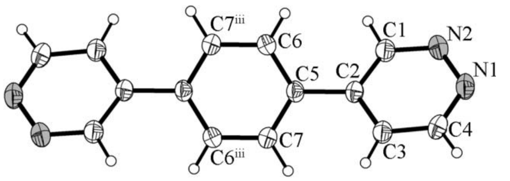

Figure 1
The structure of (I), showing the atom-labeling scheme. Displacement ellipsoids are drawn at the 35% probability level, H atoms are shown as small spheres of arbitrary radii and N atoms are shaded gray. [Symmetry code: (iii) $-x+2, -y+2, -z+1$.]

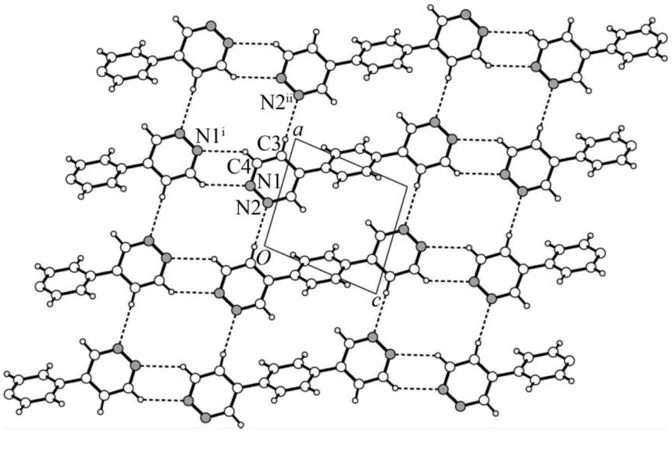

Figure 2
A projection of the structure of (I) on to the *ac* plane, showing weak C—H···N hydrogen-bonding interactions as dashed lines. N atoms are shaded gray. [Symmetry codes: (i) $-x+1, -y+1, -z-1$; (ii) $x+1, y, z$.]

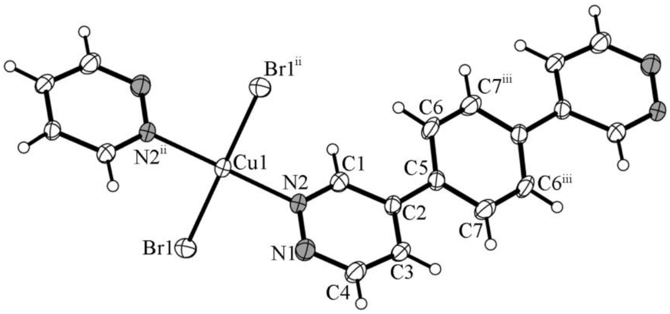

Figure 3
The structure of (II), showing the atom-labeling scheme. Displacement ellipsoids are drawn at the 40% probability level, H atoms are shown as small spheres of arbitrary radii and N atoms are shaded gray. [Symmetry codes: (ii) $-x, -y, -z$; (iii) $-x+1, -y+1, -z$.]

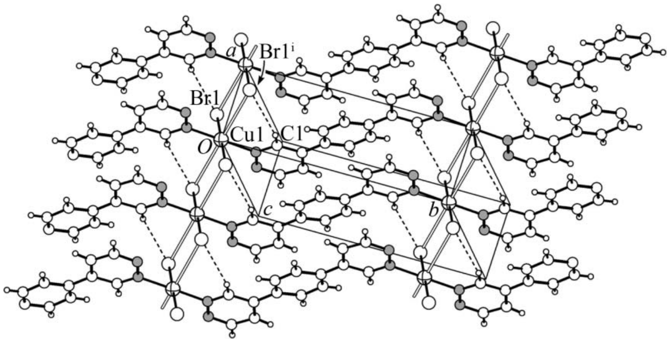

Figure 4
A fragment of the structure of (II), showing weak Cu···Br coordination (open lines) and C—H···Br hydrogen-bonding (dashed lines) interactions between the metal–organic chains. N atoms are shaded gray. [Symmetry code: (i) $-x+1, -y, -z$.]

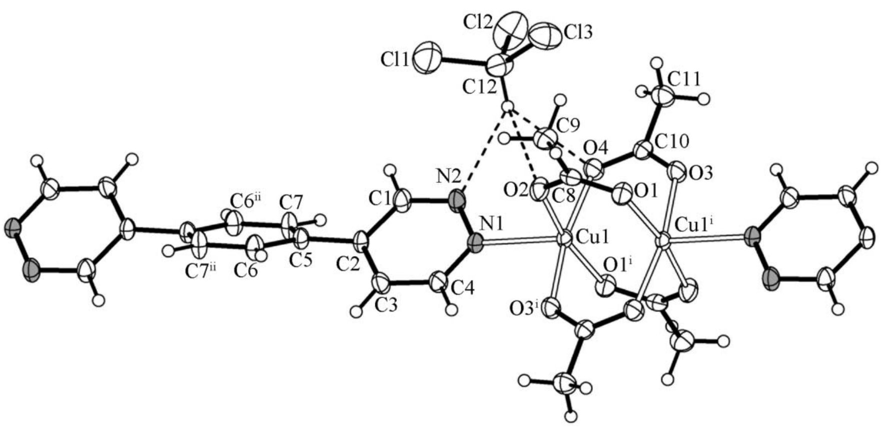

Figure 5
The structure of (III), showing the atom-labeling scheme. Displacement ellipsoids are drawn at the 40% probability level, H atoms are shown as small spheres of arbitrary radii and N atoms are shaded gray. Coordination bonds are shown with open lines and the trifurcated hydrogen bonding is indicated by dashed lines. [Symmetry codes: (i) $-x + 1, -y + 1, -z + 1$; (ii) $-x - 1, -y, -z$.]

Cu···Br contacts are accompanied also by weak C1—H1···Br1^{i} hydrogen bonding [C···Br = 3.449 (4) Å and C—H···Br = 133°; Desiraju & Steiner, 1999].

The crystal structure of (III) is based on very characteristic dicopper(II)–tetraacetate units, which are situated across a center of inversion [Cu1···Cu1^{i} = 2.6332 (7) Å; symmetry code: (i) $-x + 1, -y + 1, -z + 1$; Fig. 5]. The ligands act as N^1,$N^{1'}$-bidentate linear bridges connecting these $Cu_2(AcO)_4$ units into rod-like linear chains, with a separation between the dinuclear unit centroids of 18.2164 (13) Å. This motif is similar to that found for a related 4,4′-bipyridazine complex (Domasevitch, Gural'skiy *et al.*, 2007). The copper ions adopt tetragonal pyramidal coordination, with four basal acetate O atoms [Cu—O = 1.960 (2)–1.975 (2) Å] and pyridazine atom N1 at the apex [2.199 (2) Å]. The latter separation is consistent with the Cu—N bond length for the orthorhombic polymorph of tetraacetatodipyridinedicopper(II) [2.191 (2) Å; Uekusa *et al.*, 1989].

The uncoordinated N atoms (N2) also function as acceptors of hydrogen bonding and, together with two adjacent carboxylate atoms (O2 and O4), they provide three-center acceptor sites for the accommodation of chloroform solvent molecules. The latter are held between the coordination chains (Fig. 6) and interact with them by means of weak trifurcated hydrogen bonding [C12—H12···O(N) = 3.298 (5)–3.541 (4) Å and 130–138°; Table 5 and Fig. 5]. Comparable trifurcated hydrogen bonding is known for chloroform solvates of molecular metal complexes such as tris(1-hydroxy-2-pyridinethionato-*O*,*S*)cobalt(III) (C—H···O = 3.07–3.39 Å; Manivannan *et al.*, 1993). However, this supramolecular pattern is unprecedented for pyridazine and related polynitrogen heterocycles, and it may be relevant for functionalization of the metal–organic structure towards specific interactions with the guest species.

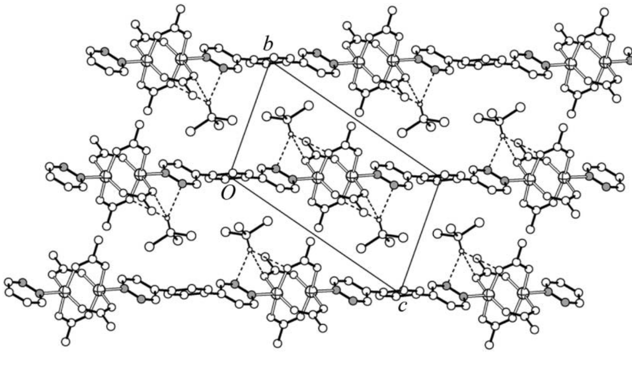

Figure 6
A projection of the structure of (III) on to the *bc* plane, showing the mode of incorporation of hydrogen-bonded chloroform molecules between the coordination chains. N atoms are shaded gray and the coordination bonds are shown with open lines.

There are no π–π or C—H···π contacts in (II) and (III), and no C—H···π bonding in (I). Thus, the inherent electron deficiency of the pyridazine ring actually appears to preclude the formation of hydrogen bonds involving π acceptors. Such closely packed motifs supported by extensive C—H···π bonding are typical for lengthy aromatic ligands (Domasevitch *et al.*, 2002), and they mitigate the formation of open structures. From this point of view, the combination of heterocyclic functions and carbocyclic spacer provided by 4,4′-(*p*-phenylene)bipyridazine could be especially favorable for the preparation of open metal–organic frameworks.

Experimental

The ligand was synthesized by reacting 1,2,4,5-tetrazine (2.30 g, 28 mmol) and 1,4-diethynylbenzene (1.76 g, 14 mmol) in dry 1,4-dioxane (40 ml, 24 h, 353 K). The yield of pure colorless crystalline product was 2.95 g (90%). For the synthesis of (II), $CuBr_2$ (11.1 mg, 0.05 mmol), (I) (11.7 mg, 0.05 mmol) and water (5 ml) were sealed in a Pyrex tube, heated at 443 K for 8 h, and then cooled to room temperature over a period of 48 h. This afforded green prisms of (II) (yield: 90%, 20.5 mg). Complex (III) was synthesized using the layering technique; a solution of $Cu(AcO)_2 \cdot H_2O$ (16.0 mg, 0.08 mmol) in methanol (3 ml) was layered over a solution of (I) (9.4 mg, 0.04 mmol) in a mixture of methanol (2 ml) and chloroform (2 ml). Large green–blue prisms of (III) grew on the walls of the tube as the solutions interdiffused over a period of 15 d (yield: 65%, 21.7 mg).

Compound (I)

Crystal data

$C_{14}H_{10}N_4$
M_r = 234.26
Triclinic, $P\bar{1}$
a = 6.3588 (7) Å
b = 6.9307 (9) Å
c = 7.0681 (10) Å
α = 110.282 (3)°
β = 90.823 (3)°
γ = 106.585 (2)°
V = 277.80 (6) Å^3
Z = 1
Mo $K\alpha$ radiation
μ = 0.09 mm^{-1}
T = 296 (2) K
0.26 × 0.23 × 0.20 mm

m256 Degtyarenko et al. • $C_{14}H_{10}N_4$, $[CuBr_2(C_{14}H_{10}N_4)]$ and $[Cu_2(C_2H_3O_2)_4(C_{14}H_{10}N_4)]\cdot 2CHCl_3$ Acta Cryst. (2008). C64, m254–m258

Data collection

Siemens SMART CCD area-detector diffractometer
2129 measured reflections
1131 independent reflections
894 reflections with $I > 2\sigma(I)$
$R_{\rm int} = 0.028$

Refinement

$R[F^2 > 2\sigma(F^2)] = 0.050$
$wR(F^2) = 0.137$
$S = 1.10$
1131 reflections
102 parameters
All H-atom parameters refined
$\Delta\rho_{\rm max} = 0.30$ e Å^{-3}
$\Delta\rho_{\rm min} = -0.18$ e Å^{-3}

Table 1
Selected bond lengths (Å) for (I).

N1—C4	1.327 (3)	C2—C3	1.376 (3)
N1—N2	1.345 (2)	C2—C5	1.482 (2)
N2—C1	1.325 (2)	C3—C4	1.387 (2)
C1—C2	1.393 (3)		

Table 2
Hydrogen-bond geometry (Å, °) for (I).

D—H···*A*	*D*—H	H···*A*	*D*···*A*	*D*—H···*A*
C4—H4···N1$^{\rm i}$	0.91 (2)	2.66 (2)	3.399 (3)	139 (2)
C3—H3···N2$^{\rm ii}$	0.96 (2)	2.65 (2)	3.608 (2)	175 (2)

Symmetry codes: (i) $-x+1, -y+1, -z-1$; (ii) $x+1, y, z$.

Compound (II)

Crystal data

[CuBr$_2$(C$_{14}$H$_{10}$N$_4$)]
$M_r = 457.62$
Monoclinic, $P2_1/c$
$a = 4.1377$ (2) Å
$b = 12.5407$ (7) Å
$c = 13.5301$ (8) Å
$\beta = 93.786$ (4)°
$V = 700.54$ (7) Å^3
$Z = 2$
Mo *Kα* radiation
$\mu = 7.26$ mm^{-1}
$T = 296$ (2) K
0.24 × 0.20 × 0.19 mm

Data collection

Siemens SMART CCD area-detector diffractometer
Absorption correction: empirical (using intensity measurements) (*SADABS*; Sheldrick, 1996)
$T_{\rm min} = 0.203$, $T_{\rm max} = 0.251$
3750 measured reflections
1415 independent reflections
1099 reflections with $I > 2\sigma(I)$
$R_{\rm int} = 0.031$

Refinement

$R[F^2 > 2\sigma(F^2)] = 0.031$
$wR(F^2) = 0.070$
$S = 1.06$
1415 reflections
97 parameters
H-atom parameters constrained
$\Delta\rho_{\rm max} = 0.54$ e Å^{-3}
$\Delta\rho_{\rm min} = -0.37$ e Å^{-3}

Table 3
Selected geometric parameters (Å, °) for (II).

Cu1—N2	2.005 (3)	Cu1—Br1$^{\rm i}$	3.2421 (4)
Cu1—Br1	2.4151 (4)		
N2—Cu1—Br1$^{\rm ii}$	90.57 (9)	N2—Cu1—Br1$^{\rm i}$	88.40 (9)
N2—Cu1—Br1	89.43 (9)	Br1—Cu1—Br1$^{\rm i}$	87.158 (12)
C1—C2—C5—C6	12.6 (5)		

Symmetry codes: (i) $-x+1, -y, -z$; (ii) $-x, -y, -z$.

Compound (III)

Crystal data

[Cu$_2$(C$_2$H$_3$O$_2$)$_4$(C$_{14}$H$_{10}$N$_4$)]·2CHCl$_3$
$M_r = 836.25$
Triclinic, $P\overline{1}$
$a = 7.6349$ (8) Å
$b = 8.0203$ (8) Å
$c = 13.9312$ (10) Å
$\alpha = 104.601$ (2)°
$\beta = 103.993$ (2)°
$\gamma = 90.123$ (3)°
$V = 799.21$ (13) Å^3
$Z = 1$
Mo *Kα* radiation
$\mu = 1.88$ mm^{-1}
$T = 296$ (2) K
0.27 × 0.15 × 0.12 mm

Data collection

Siemens SMART CCD area-detector diffractometer
Absorption correction: empirical (using intensity measurements) (*SADABS*; Sheldrick, 1996)
$T_{\rm min} = 0.630$, $T_{\rm max} = 0.805$
8062 measured reflections
3283 independent reflections
2688 reflections with $I > 2\sigma(I)$
$R_{\rm int} = 0.035$

Refinement

$R[F^2 > 2\sigma(F^2)] = 0.040$
$wR(F^2) = 0.090$
$S = 1.07$
3283 reflections
201 parameters
H-atom parameters constrained
$\Delta\rho_{\rm max} = 0.34$ e Å^{-3}
$\Delta\rho_{\rm min} = -0.41$ e Å^{-3}

Table 4
Selected geometric parameters (Å, °) for (III).

Cu1—O1$^{\rm i}$	1.960 (2)	Cu1—O3$^{\rm i}$	1.975 (2)
Cu1—O4	1.967 (2)	Cu1—N1	2.199 (2)
Cu1—O2	1.969 (2)	Cu1—Cu1$^{\rm i}$	2.6332 (7)
O1$^{\rm i}$—Cu1—O4	88.70 (9)	O2—Cu1—O3$^{\rm i}$	90.12 (9)
O1$^{\rm i}$—Cu1—O2	168.03 (9)	O1$^{\rm i}$—Cu1—N1	101.31 (9)
O4—Cu1—O2	88.73 (9)	O4—Cu1—N1	101.53 (9)
O1$^{\rm i}$—Cu1—O3$^{\rm i}$	89.99 (9)	O2—Cu1—N1	90.66 (9)
O4—Cu1—O3$^{\rm i}$	168.07 (8)		
C1—C2—C5—C7	44.1 (5)		

Symmetry code: (i) $-x+1, -y+1, -z+1$.

Table 5
Hydrogen-bond geometry (Å, °) for (III).

D—H···*A*	*D*—H	H···*A*	*D*···*A*	*D*—H···*A*
C12—H12···O2	0.98	2.83	3.541 (4)	130
C12—H12···O4	0.98	2.50	3.298 (5)	138
C12—H12···N2	0.98	2.71	3.496 (5)	137

For (I), all H atoms were found in intermediate difference Fourier maps and were refined fully with isotropic displacement parameters [C—H = 0.91 (2)–0.99 (2) Å]. For (II) and (III), the H atoms were treated as riding in geometrically idealized positions, with aromatic C—H distances of 0.93 Å, methyl C—H distances of 0.96 Å and chloroform C—H distances of 0.98 Å, and with $U_{\rm iso}$(H) values of 1.2$U_{\rm eq}$(C) or 1.5$U_{\rm eq}$(methyl C).

For all compounds, data collection: *SMART-NT* (Bruker, 1998); cell refinement: *SAINT-NT* (Bruker, 1999); data reduction: *SAINT-NT*; program(s) used to solve structure: *SHELXS97* (Sheldrick, 2008); program(s) used to refine structure: *SHELXL97* (Sheldrick, 2008); molecular graphics: *DIAMOND* (Brandenburg, 1999); software used to prepare material for publication: *WinGX* (Farrugia, 1999).

This work was supported in part by a grant from Deutsche Forschungsgemeinschaft (UKR 17/1/06 to KVD).

Supplementary data for this paper are available from the IUCr electronic archives (Reference: HJ3079). Services for accessing these data are described at the back of the journal.

References

Baudour, J. L., Toupet, L., Délugeard, Y. & Ghémid, S. (1986). *Acta Cryst.* C**42**, 1211–1217.

Blake, A. J. & Rankin, D. W. H. (1991). *Acta Cryst.* C**47**, 1933–1936.

Brandenburg, K. (1999). *DIAMOND*. Release 2.1e. Crystal Impact GbR, Bonn, Germany.

Bruker (1998). *SMART-NT*. Version 5.0. Bruker AXS Inc., Madison, Wisconsin, USA.

Bruker (1999). *SAINT-NT*. Version 6.02. Bruker AXS Inc., Madison, Wisconsin, USA.

Carlucci, L., Ciani, G., Moret, M. & Sironi, A. (1994). *J. Chem. Soc. Dalton Trans.* pp. 2397–2404.

Desiraju, G. R. & Steiner, T. (1999). *The Weak Hydrogen Bond in Structural Chemistry and Biology*, pp. 29–120. New York: Oxford University Press.

Domasevitch, K. V., Gural'skiy, I. A., Solntsev, P. V., Rusanov, E. B., Krautscheid, H., Howard, J. A. K. & Chernega, A. N. (2007). *Dalton Trans.* pp. 3140–3148.

Domasevitch, K. V., Sieler, J., Rusanov, E. B. & Chernega, A. N. (2002). *Z. Anorg. Allg. Chem.* **628**, 51–56.

Domasevitch, K. V., Solntsev, P. V., Gural'skiy, I. A., Krautscheid, H., Rusanov, E. B., Chernega, A. N. & Howard, J. A. K. (2007). *Dalton Trans.* pp. 3893–3905.

Farrugia, L. J. (1999). *J. Appl. Cryst.* **32**, 837–838.

Fetzer, T., Lentz, A., Debaerdemaeker, T. & Abou-El-Wafa, O. (1990). *Z. Naturforsch. Teil B*, **45**, 199–202.

Janiak, C. (2000). *J. Chem. Soc. Dalton Trans.* pp. 3885–3898.

Manivannan, V., Dutta, S., Basu, P. & Chakravorty, A. (1993). *Inorg. Chem.* **32**, 769–771.

Morosin, B. (1975). *Acta Cryst.* B**31**, 632–634.

Otieno, T., Rettig, S. J., Thompson, R. C. & Trotter, J. (1995). *Inorg. Chem.* **34**, 1718–1725.

Sauer, J., Heldmann, D. K., Hetzenegger, J., Krauthan, J., Sichert, H. & Schuster, J. (1998). *Eur. J. Org. Chem.* **1**, 2885–2896.

Schmidt, M. W., Baldridge, K. K., Boatz, J. A., Elbert, S. T., Gordon, M. S., Jensen, J. H., Koseki, S., Matsunaga, N., Nguyen, K. A., Su, S., Windus, T. L., Dupuis, M. & Montgomery, J. A. (1993). *J. Comput. Chem.* **14**, 1347–1363.

Sheldrick, G. M. (1996). *SADABS*. University of Göttingen, Germany.

Sheldrick, G. M. (2008). *Acta Cryst.* A**64**, 112–122.

Uekusa, H., Ohba, S., Saito, Y., Kato, M., Tokii, T. & Muto, Y. (1989). *Acta Cryst.* C**45**, 377–380.